ELSEVIER

Journal of Hazardous Materials 44 (1995) 209–230

JOURNAL OF HAZARDOUS MATERIALS

Reassessment and reevaluation of rainout and drop size correlation for an aerosol jet

John L. Woodward[a,*], Antonis Papadourakis[b]

[a] *DNV Technica Inc., 355 E. Campus View Blvd., Suite 170, Columbus, OH 43235, USA*
[b] *Rohm and Haas Co., P.O. Box 584, Bristol, PA 19007, USA*

Received 10 September 1994; accepted 7 April 1995

Abstract

A number of aerosol rainout experiments were conducted in Oklahoma in 1989 and in Nevada in 1990 using five superheated, flashing liquids. Since some of these liquids were relatively volatile, the rained out liquid was imperfectly captured; evaporation from the capture pans was evident. This paper describes an approach to correct the rainout data for reevaporation using a model of all the pertinent phenomena involved. Corrected rainout fractions are provided for chlorine, methylamine, and cyclohexane.

The model used requires adjusting only two variables, solubility for capture in aqueous solution, and the initial mean drop size. Adjusting the mean drop size for each experiment provides a set of drop sizes which can then be tested against alternative drop size correlation variables. Desirable correlations force overlap between all five materials tested and have the correct behavior with overpressure. Acceptable correlations are found between drop size and superheat, partial expansion energy, and an extended flash fraction. With two different slopes bubble growth rate also provides a good correlation. Unacceptable correlation occurred using Jacob number, flash fraction, and expansion energy.

Keywords: Aerosol modeling; Drop size; Rainout; Dispersion modeling

1. Introduction

A major proportion of the available data for aerosol rainout has been obtained by experiments sponsored by the Center for Chemical Process Safety (CCPS) of the American Institute of Chemical Engineers (AIChE) and the US Department of Energy. These data are reported in two reports [1, 2], and in a summary paper by Johnson [3]. Five materials were tested (in order of decreasing volatility): chlorine,

* Corresponding author. Tel.: 614-848 4000. Fax: 614-848 3955.

0304-3894/95/$09.50
SSDI 0304-3894(95)00055-0

monomethylamine, CFC-11, cyclohexane, and water. During the tests and in analyses soon thereafter it was recognized that the observed capture fractions did not represent the entire rainout fraction because of evaporation from the capture pans. Consequently, CCPS sponsored reevaluation of these data to calculate the evaporation occurring and to correct the reported rainout fractions. Corrected rainout data are reported here for chlorine, monomethylamine, and cyclohexane.

A model of aerosol behavior applicable to these tests must be able to predict not only drop size, plume and droplet trajectories, air entrainment to the aerosol plume, and heat and mass transfer rates to the droplets, but also reevaporation and solution rates into the capture liquid. In an accompanying paper [4] we describe such a model, the Unified Dispersion Model (UDM), and its experimental basis. With the UDM liquid rainout predictions are a sensitive function of the initial drop size. In reconciling the CCPS rainout test data, an initial Sauter mean average drop size is found for each experiment. These values are used here with various correlating variables to find the correlation which best represents the drop sizes found for all five test materials.

2. Experimental methodology of CCPS tests

The experimental work in the CCPS tests used a source tank which could be heated to various degrees of superheat and pressurized with a nitrogen blanket to various degrees of overpressure (above the vapor pressure). As depicted in Fig. 1, the source tank was mounted on load cells and mass discharge rates were derived from the time trace of the tank mass. Discharge was horizontal, 1.22 m above the surface of the capture pans, which were 50′ long and 20′ wide in five 10′ long segments.

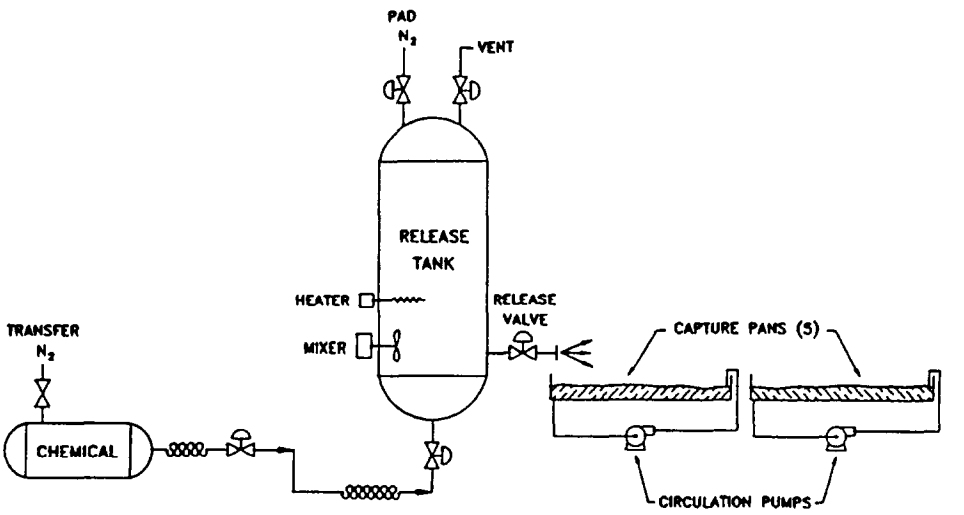

Fig. 1. Schematic of setup for rainout experiments. (Reproduced by permission of CCPS).

For cyclohexane, CFC-11 and water, the captured liquid drained to a bucket which was weighed. For chlorine and methylamine releases the capture pans contained a caustic solution, or an acid solution, respectively. Capture was determined by titration of the solutions. For cyclohexane, the pans were crudely cooled by a water spray directed at the bottom of the pans.

For the water and CFC-11 tests, the source tank and capture pans were in a semi-cylindrical tunnel, open at the ends, made up of plastic sheeting over a frame. Details of the experimental approach are in the CCPS reports [1, 2].

3. Reasons for suspicion of the rainout data

Reevaporation of the volatile chlorine rainout is evident from the videotape records of these tests. Reevaporation was also evident in the earliest cyclohexane tests when the capture pans had no cooling by water spray. With the capture pans heated in the summer Nevada sun, the captured liquid evaporated completely!

Fig. 2 provides additional reason to infer reevaporation. This figure was reported previously [5] using the uncorrected rainout data (taking the capture fraction as the

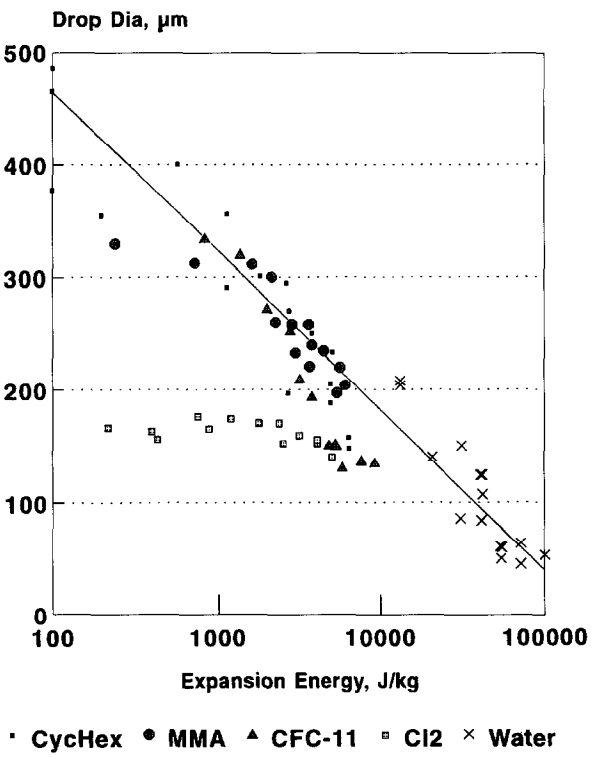

Fig. 2. Drop size adjusted to match uncorrected rainout (capture) fraction as a function of expansion energy.

rainout fraction). An earlier version of the UDM was used to predict the rainout fraction for each experiment. The drop size required for the predicted rainout fraction to match the observed capture fraction is plotted against the expansion energy defined along an isentropic expansion path as

$$E_{EXP} = \Delta H|_S - (P_o - P_a)v_o.$$

Only data with low (< 60 kPa) overpressure are plotted. Fig. 2 shows that the required drop sizes substantially overlap along a single correlating line with two exceptions. The chlorine drop sizes depart from the trend line, more so at lower expansion energies which correspond to low superheat. Similarly, the methylamine data with low expansion energy and superheat fall below the trend line. Correcting the chlorine and methylamine data for evaporation brings the required drop sizes up to the trend line as is shown later.

4. Modeling solution rates into aqueous phase

The theory for dissolution in water has been developed by analogy with that for evaporation of pools on liquid and is based upon Dodge et al. [6]. Assuming a logarithmic driving force with local solubility w_s and background concentration at infinity of w_∞ (assumed zero), the rate at which material dissolves in a pool of radius r is given by

$$\left[\frac{dm}{dt}\right]_{sol} = \pi r^2 u_w^* \rho_w Da^* \ln\left[\frac{1 - w_\infty}{1 - w_s}\right].$$

The solution of this equation, and the pool evaporation model is discussed in the appendix of an accompanying paper [4].

5. Correcting rainout data for chlorine and methylamine

Measured experimental conditions are summarized in Tables 1 and 2 for the chlorine and methylamine experiments and in CCPS reports [2, 7]. There is little variation in ambient temperature and relative humidity, and only moderate variation in wind speed in these tests. Ambient pressure was essentially constant.

The mass balance for each test must satisfy:

$$m_{rel} = m_{de} + m_{pe} + m_{cap},$$

where m_{rel} is the $w\Delta t$ = mass discharged, m_{de} is the mass evaporated by flashing and by drops evaporating in flight, m_{pe} is the mass evaporating from capture pan, and m_{cap} is the mass captured (dissolved or collected). The mass evaporated in flight includes the flash fraction. Of these, m_{rel} and m_{cap} are observed values, m_{de} is predicted by the

Table 1
Experimental data for chlorine releases (P_{amb} = 90.3 kPa, T_{sat} = 236.59 K at this pressure, Orifice diam. = 6.35 mm)

Test number[a]	Disch. temp.[b] (K)	Disch. press.[b] (kPa)	Disch. rate[a] (kg/s)	Liquid[a] capture (%)	Drop diam. (μm)	Predicted % dissolving	Predicted capture (m%)	Corrected rainout (m%)
1	247.4	178.9	0.382	23.4	407	35.3	23.4	66.1
2	250.9	215.5	0.440	20.2	319	35.6	20.2	56.7
3	251.5	225.9	0.443	17.1	277	32.8	17.1	50.6
4	256.4	257.0	0.487	21.5	370	36.3	21.5	59.0
5	258.1	258.6	0.485	16.6	267	35.4	16.6	47.0
6	261.8	303.3	0.552	18.1	297	35.5	18.1	51.0
7	267.4	358.6	0.604	16.2	272	36.6	16.2	44.3
8	272.4	420.8	0.645	15.2	262	36.1	15.2	42.2
9	273.3	433.9	0.652	9.6	206	31.2	9.6	30.7
10	277.9	482.3	0.704	9.0	196	35.8	9.0	25.1
11	283.6	567.2	0.758	3.9	183	35.0	3.8	10.8
12	283.7	558.9	0.742	5.3	187	36.0	5.3	14.6
13	289.2	661.1	0.834	1.3	150	34.5	1.3	3.8
14	245.4	183.7[c]	0.39	16.5	264	36.2	16.5	45.5
15	247.1	178.9	0.38	18.9	290	35.7	19.0	53.2
16	261.3	586.0	0.81	11.7	197	35.6	11.9	25.0
17	261.8	922.5	1.05	6.8	182	35.7	6.7	14.2
18	267.1	639.1	0.84	9.2	154	35.4	9.2	26.0
19	267.1	979.1	1.07	4.1	190	36.5	4.1	8.4
20	267.6	295.9[c]	0.45	13.2	253	36.5	13.2	36.3
21	272.8	382.2	0.51	16.6	292	36.9	16.5	44.9
22	278.1	417.5[c]	0.54	8.1	204	35.7	8.0	22.5

[a] From Johnson [3] Table 4.
[b] From Quest [2] Table 5.2.
[c] Raised to vapor pressure.

drop evaporation model, and m_{pe} is predicted by the pool evaporation and dissolution model. Utilizing the remaining two degrees of freedom we can match observed capture data be adjusting the initial drop size to change m_{de} and the solubility, w_s, to change m_{pe}. An approach to do this is outlined below, resulting in corrected rainout fractions summarized in Tables 1 and 2 and plotted in Figs. 3 and 4. Clearly, larger corrections are required for chlorine than for methylamine.

Also listed in Tables 1 and 2 is the percent of rained out liquid dissolving in the capture fluid:

$$100\, m_{cap}/(m_{pe} + m_{cap}).$$

This ratio is seen to be essentially constant for each material. This occurs because the heat and mass transfer coefficients below the water surface are both evaluated with a common correlation variable, the Dalton number, and with a common driving force set by the effective solubility of chlorine in caustic solution or methylamine in acid solution, w_s.

Table 2
Experimental data for methylamine releases (P_{amb} = 90.3 kPa, T_{sat} = 264.26 K at this pressure, Orifice diam. = 6.35 mm unless otherwise noted)

Test no.	Discharge temp (K)	Disch. press. (kPa)	Disch. rate (kg/s)	Liquid capture (m%)	Drop diam. (μm)	Pred. % dissolving	Pred. capture (%)	Corrected rainout (m%)
1	270.4	170.7	0.247	54.8	430	89.4	54.8	61.3
2	275.0	196.1	0.276	50.2	400	89.4	50.3	56.2
3	280.4	233.3	0.305	47.6	398	89.3	47.6	53.3
4	282.9	256.1	0.321	44.9	378	89.4	45.0	50.3
5[a]	283.3	248.9	1.246	39.9	243	87.7	39.9	45.5
6	285.8	283.7	0.350	34.7	268	89.4	22.37	25.0
7	286.3	297.5	0.359	27.2	288	89.3	27.2	30.4
8	288.5	297.5	0.354	36.0	302	89.3	35.9	40.2
9[a]	288.7	291.3	1.368	34.5	227	79.0	34.5	43.7
10	288.9	304.4	0.360	30.4	288	89.4	30.7	34.4
11	291.2	334.1	0.377	28.2	279	89.4	28.35	31.7
12	293.8	356.1	0.400	20.7	217	85.7	20.5	23.9
13[a]	294.6	356.1	1.534	27.5	193	84.3	27.5	32.6
14	295.7	378.9	0.405	17.9	238	89.2	17.8	20.0
15	285.8	559.5	0.517	22.2	270	89.4	22.2	24.8
16	286.1	209.9[b]	0.268	26.9	297	89.2	27.1	30.4
17	288.5	227.2[b]	0.284	51.0	427	89.3	50.3	56.3
18	288.7	263.7	0.328	40.7	320	89.4	40.9	45.8

[a] Orifice diam. = 12.7 mm.
[b] Raised to vapor pressure in discharge modeling.

Higher values of w_s increase m_{cap} and decrease m_{pe}. In order to keep the capture fraction matching observed data with this change, the rainout fraction must decrease, so m_{de} must increase. The only adjustable variable which affects m_{de} is the initial mean drop size which must decrease. Thus, an increase in solubility requires smaller initial drop sizes for all chlorine and methylamine tests, and vice versa. The solubility values used are 0.20 kg/kg for chlorine and 0.36 kg/kg for methylamine. These values force the chlorine and methylamine drop sizes to be in line with drop sizes found for the other three materials. The solubility of chlorine in neutral pH water at 25 °C is 0.868 kg Chlorine/kg solution [8]. For methylamine, the solubility at 25 °C is 0.556 kg/kg [8]. Clearly, the modeled values indicate that some mass transfer resistance is being modeled by the driving force term (the solubility) that should be modeled by the mass transfer coefficient correlations.

6. Correcting rainout data for cyclohexane

Experimental data for cyclohexane are summarized in Table 3. The observed capture data must be corrected for evaporation in the capture pans from the combined effects of solar radiation, convection from the air, and conduction from the capture pans.

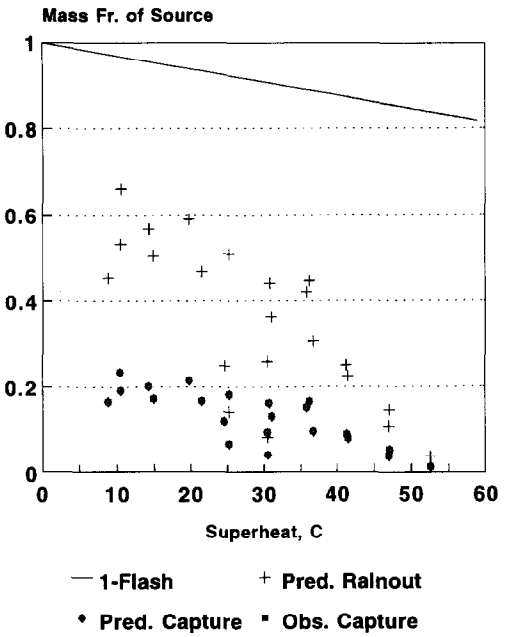

Fig. 3. Chlorine rainout corrected for solution and evaporation.

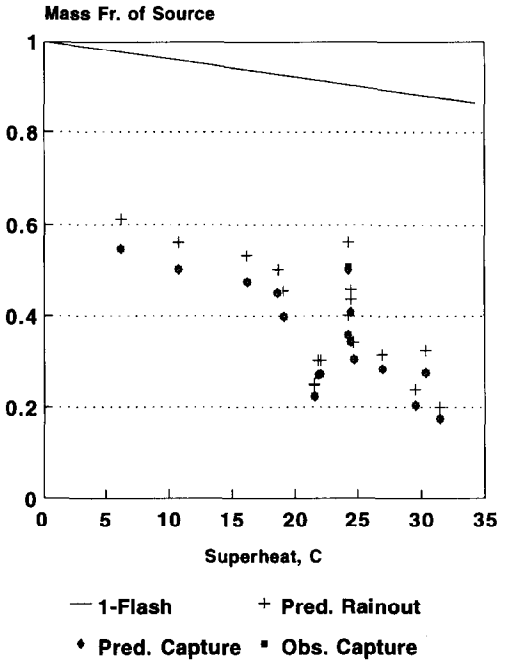

Fig. 4. Methylamine rainout corrected for solution and evaporation.

Table 3
Experimental data for cyclohexane releases (P_{amb} = 90.3 kPa, T_{sat} = 350.1 K at this pressure, Orifice diam. = 6.35 mm)

Test number	Discharge temp. (K)	Discharge press. (kPa)	Discharge rate (kg/s)	Liquid capture[a] (%)	Drop diam. (μm)	Rainout liq. temp. (K)	Ave. evap. rate from rainout model (kg/s)	Corrected rainout (%)
1	353.7	182.9	0.260	53.4	377	268.5	0.0193	48.1
2	359.9	209.1	0.283	51.7	355	267.8	0.0146	45.6
3	365.2	217.4	0.300	53.5	400	268.1	0.0145	46.7
4	370.9	239.5	0.315	38.4	290	268.0	0.0142	33.7
5	376.1	256.0	0.331	44.1	301	267.7	0.0165	36.1
6	382.1	282.9	0.357	33.4	270	268.3	0.0191	26.7
7	387.4	309.9	0.375	32.1	251	267.6	0.0152	24.6
8	392.8	354.7	0.406	17.6	188	267.1	0.0082	9.53
9	398.2	383.7	0.414	10.3	148	270.9	0.0002	0.05
10	398.4	391.9	0.428	9.5	157	266.3	0.0073	5.83
11	337.6	142.1	0.211	71.0	485	269.1	0.0140	64.4
12	343.3	140.1	0.199	70.6	485	269.4	0.0147	62.4
13	348.3	140.8	0.203	69.3	465	267.1	0.0154	58.7
14	369.1	156.0	0.222	69.2	630	272.5	0.0263	54.9
15	370.7	192.6	0.272	47.6	356	269.7	0.0267	38.7
16	381.3	251.2	0.326	31.9	294	269.5	0.0213	26.78
17	381.3	213.3	0.288	53.0	381	268.3	0.0219	41.1
18	382.9	556.0	0.533	17.5	197	267.9	0.0097	9.94
19	392.5	274.0	0.346	24.7	234	269.3	0.0121	13.18
20	392.9	318.2	0.378	23.9	206	268.2	0.0125	12.1
EV[b]	303.0	140.0	0.755	—	—	—	—	—

[a] These values are corrected for evaporation rate by Quest.
[b] The discharge temperature, pressure and duration are assumed. The discharge rate is calculated for a 12.7 mm orifice.

Solar radiation data were acquired from the National Solar Radiation Data Base [9] for the nearest measurement site at Las Vegas, Nevada for the period of the cyclohexane tests, 7–11 September 1990. Part of these data are plotted in Fig. 5. Also shown, as the dashed curve, is a half sine wave, showing that the data are not exactly sinusoidal, even allowing for perturbations caused by cloud cover and atmospheric disturbances. Even so, we interpolated through each test period by fitting a sine wave through the observed radiation for the hours before and after each test. We then integrated this curve between the start and stop of each test to obtain an average over the test period.

An experiment was conducted by Quest [2] to evaluate the evaporation rate of cyclohexane by irrigating it across the capture pan while the pan was cooled from the bottom side with a water spray. An average evaporation rate found from this test is E_T = 0.039 kg/s. By analyzing videotape records, the maximum wetted area was found for each cyclohexane experiment, as well as for the evaporation rate experiment.

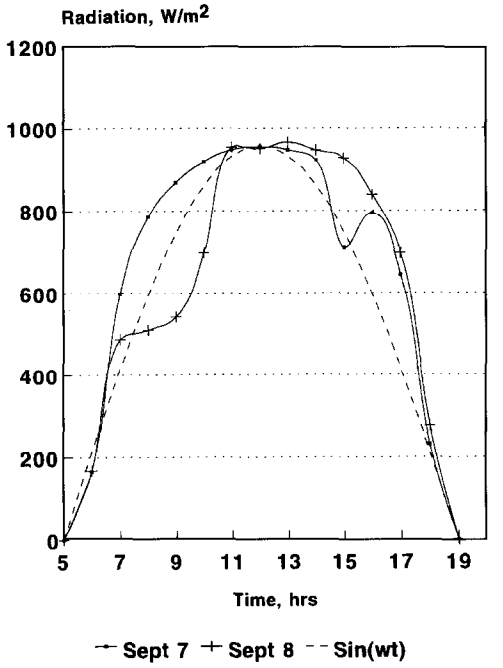

Fig. 5. Solar radiation in Las Vegas, NV in September 1990.

The test duration is not reported, but is assumed to be 300 s. The discharge rate is also not given, and is assumed to range from 0.35 to 0.50 kg/s.

Applying the pool evaporation model to the evaporation rate experiment we obtained the predicted evaporation rates shown in Fig. 6. Since the pan temperature was not measured, we used three values for this, 303, 306, 310 K (30, 33, 37 °C), of which 310 K is the ambient temperature for the test. The predicted evaporation rate is seen to increase as long as fresh, warm cyclohexane continues to be injected to the pool. When the injection stops, the pool temperature and pool evaporation rate drop, trending toward a nearly steady-state condition which balances heat input rate with heat loss by evaporation. Taking an average across the predicted time-varying evaporation rate of ± 2 min from the time the injection stops gives an average evaporation rate of 0.038 kg/s with the substrate temperature equal to ambient temperature. This is for 0.35 kg/s discharge rate. With 0.50 kg/s discharge rate the average predicted evaporation rate is 0.0407 kg/s. Since these values bracket the observed value, this is taken as confirmation of the evaporation model.

Since injection was by irrigation, the temperature of the cyclohexane used in the evaporation rate test is very nearly the saturation temperature (boiling point). In the rainout tests where the source was elevated, the droplet temperatures were observed to decrease substantially. This temperature decrease is predicted by our model and is found to decrease average evaporation rates substantially below the value found in the irrigation experiment.

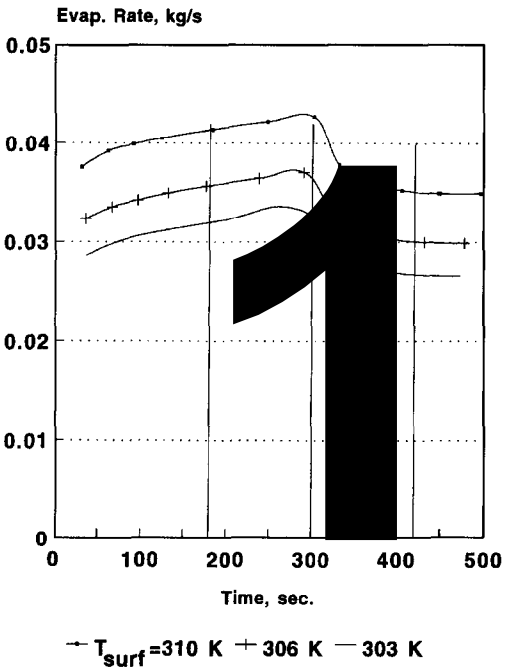

Fig. 6. Predicted evaporation rates for cyclohexane flowing across a metal capture pan in the Nevada tests. The capture pan is cooled with a water spray under the collection surface so the pan temperature is assumed. Setting the pan temperature to the ambient temperature, 301 K, gives an average evaporation over a four minute period nearest the observed value of 0.039 kg/s.

Table 3 shows the corrections made to cyclohexane rainout rates. The predicted liquid temperature at rainout is seen to be substantially cooled. The predicted average rainout rates are 40–50% of the previously estimated rates [2]. Quest developed these estimates simply by proportioning the wetted area of each test and by applying a wind speed adjustment to the evaporation rate found in the irrigation test. The decreased droplet temperature obtained with our model is largely responsible for the smaller evaporation rates. Fig. 7 plots the corrected rainout rates. The correction is seen to vary from test to test, largely dependent on wind speed. (Low wind speeds require small corrections for evaporation rate.)

7. Drop size correlation for flashing regime with corrected rainout data

Three drop breakup regimes are often defined [10]: capillary, aerodynamic, and flashing. The capillary breakup regime occurs only for smooth-orifices or pipes of very small diameter. For subcooled liquid discharges and even for liquids with a small degree of superheat, breakup occurs by an aerodynamic, mechanical mechanism. This

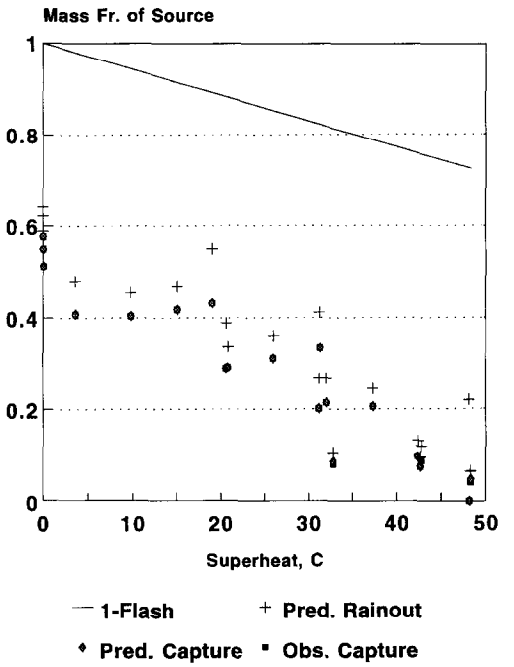

Fig. 7. Correcting cyclohexane rainout for evaporation.

is generally considered to occur when the droplet Weber number is above a critical value of around 10–15 [11]. That is:

$$We = \frac{1}{2}\frac{\rho_{air} u_o^2 d_p}{\sigma} > 10\text{–}15.$$

Superheated liquid discharges are readily seen to break up by a flashing mechanism. The vapor formed upon depressurization is modeled as emerging in bubbles which grow and ultimately interact, shattering the liquid between them. Alternative models for this regime have been suggested by Crowe and Comfort [12], Kitamura et al. [13] and Brown and York [11]. Koestel et al. [14] found a correlation for a minimum drop size making use of data by Bushnell and Gooderum [15] and Lienhard and Stephenson [16]. We develop below a correlation applicable to the flashing regime.

For risk and consequence assessment purposes, practical drop size correlations should not be entirely independent of rainout models. Thus, the drop sizes found here, being inherently linked with a practical consequence assessment model, can be particularly useful.

Some suggested correlator variables are as follows:

(1) *Superheat,*

$$\Delta T_{sh} = T_o - T_{sat}, \text{(K)}.$$

(2) *Expansion energy*, also suggested by Melhem and Saini [17]:

$$E_{exp} = -\Delta H|_S - v_o(P_o - P_a), \text{ (J/kg)}.$$

(3) *Extended flash fraction*,

$$F_p = [C_{pL}\Delta T_{sh}/h_{fg}] + v_o(P_o - P_{sat})/h_{fg}, \text{ (dimensionless)}.$$

(4) *Jacob number*

$$Ja = [C_{pL}\Delta T_{sh}/h_{fg}][\rho_L/\rho_v], \text{ (dimensionless)}.$$

(5) *Bubble growth rate*

$$C_{bub} = Ja(\pi\alpha)^{1/2}, \text{ (m/s}^{1/2}).$$

(6) *Partial expansion energy*.

$$E_p = -\Delta H|_S - v_o(P_{sat} - P_a) + v_o(P_o - P_{sat}), \text{ (J/kg)},$$

where $P_o - P_{sat}$ = overpressure.

In the expansion energy and partial expansion energy, if the ΔH term were evaluated along a constant enthalpy path, it would be zero. Along a constant entropy path, ΔH is nonzero, but small. This is seen by substituting the defining relationships for enthalpy (where T_2 is chosen to keep entropy constant):

$$H(T_2) = (1 - x_2)H_{L2} + x_2 H_{v2} \qquad H_o = H_L(T_o),$$

$$H_L = \int_{T_{ref}}^{T} C_{PL}\, T\, dT, \qquad H_{vsat} = H_L + h_{fg} + h_{ni},$$

so:

$$-\Delta H = \int_{T_o}^{T_2} C_{PL}\, T\, dT + x_2(h_{fg} + h_{ni})$$

or, using the approximation for flash fraction:

$$x_2 \cong \frac{\bar{C}_{PL}(T_o - T_2)}{h_{fg}}$$

assuming an average heat capacity and negligible nonideality:

$$-\Delta H|_S \cong \bar{C}_{PL}(T_2 - T_o) - \bar{C}_{PL}(T_2 - T_o) \cong 0.$$

With the rigorous relationship:

$$x_2 = \frac{H_L(T_o) - H_L(T_2)}{h_{fg}}$$

and rigorous enthalpy properties, the ΔH term in the expansion energy and partial expansion energy is nonzero.

The correlators, except for the expansion energy terms, exhibit a certain logical connectedness, since superheat appears in each. The questions posed by this

Table 4
Experimental data for CFC releases (P_{amb} = 97.2 kPa average, T_{sat} = 295.45 K at this pressure, Orifice diam. = 6.35 mm)

Test no.	Disch. temp. (K)	Disch. press. (kPa)	Disch. rate (kg/s)	Liquid capture (%)	Drop diam (μm)
13	289.6	168.1	0.28	61.4	363
14	295.2	166.8	0.28	59.0	338
15	297.9	161.8	0.27	61.3	450
1	308.9	163.5	0.27	62.0	550
2	314.4	190.4	0.32	51.2	362
3	319.9	224.1	0.37	51.4	362
4	324.7	254.9	0.40	47.5	332
5	327.3	269.7	0.44	32.3	253
6	330.7	302.0	0.46	30.6	220
7	336.1	343.9	0.51	10.8	156
8	338.3	362.5[a]	0.53	4.7	164
9	338.4	366.7	0.53	4.6	175
10	341.0	392.7[a]	0.54	3.8	127
11	348.8	470.6[a]	0.61	0.0	120
12	354.9	554.1	0.67	0.0	120

Release duration taken as 240 seconds; Relative humidity taken as approximately 8%.
[a] Raised to vapor pressure in calculations.

Table 5
Experimental data for water releases (P_{amb} = 96.8 kPa nominal, T_{sat} = 371.9 K at this pressure)

Test no.[a]	Disch. temp. (K)	Disch. press. (kPa)	Disch. rate (kg/s)	Orifice diam. (mm)	Liquid capture (%)	Drop diam. (μm)
1	387.7	184.5	0.70	3.2	97.0	—
2	398.7	253.1	0.354	6.4	86.0	1000
3	399.0	253.2	0.090	3.2	85.0	—
4	410.2	346.8	0.420	6.4	81.7	264
5	410.2	347.1	0.115	3.2	77.0	324
6	421.0	460.4	0.488	6.4	77.0	340
7	433.1	631.1	2.408	12.7	72.0	—
8	433.2	632.9	0.568	6.4	75.9	400
9	443.2	809.7	0.157	3.2	58.0	106
10	443.4	807.0	0.658	6.4	68.7	59
11	443.8	816.1	2.750	12.7	69.0	—
12	444.2	821.5	0.654	6.4	62.0	109
13	454.3	1047.2	0.184	3.2	61.0	38
14	454.4	1062.3	0.797	6.4	64.6	26
15	455.3	1062.0	3.111	12.7	65.0	115
16	465.7	1361.2	0.901	6.4	59.0	25
17	465.9	1352.7	0.213	3.2	58.0	18
18	476.4	1697.6	0.995	6.4	54.0	3
19	487.8	2109.4	1.144	6.4	47.0	18
20	488.2	2104.3	0.267	3.2	46.0	85

[a] From Johnson [3] Table 4.

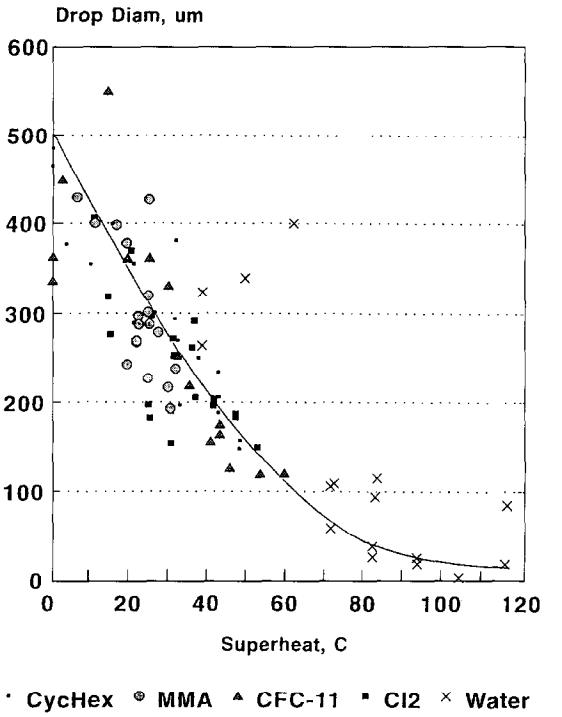

Fig. 8. Drop sizes which fit corrected rainout data as a function of superheat.

succession are:

(1) Is either superheat or expansion energy an adequate correlator?

(2) Does multiplying superheat by the liquid heat capacity, C_{PL}, and dividing by the heat of vaporization, h_{fg}, improve the correlation?

(3) In addition, does multiplying by the expansion ratio, ρ_L/ρ_v, improve the correlation?

(4) In addition, does multiplying by the term $(\pi\alpha)^{1/2}$ improve the correlation.

(5) Does the use of an additive term, $v_o(P_o - P_a)$ or $v_o(P_o - P_{sat})$ improve the correlation?

To address these questions we plotted the drop sizes listed in Tables 1–5, including those found for CFC-11 and water, in Figs. 8–12. Table 6 lists typical values of the physical properties used in the prospective correlators, each evaluated at 20 °C superheat. Table 7 shows the effect of introducing in succession the C_{pL}, h_{fg}, ρ_L/ρ_v, $(\pi\alpha)^{1/2}$. The effects of these terms are normalized to CFC-11. Ratios of terms larger than 1.0 move the data points for that material to the right of CFC-11's points, and values less than 1.0 move points to the left.

From Figs. 8–12 we observe the following:

(1) Superheat alone (Fig. 8) is a fairly good correlator for drop size. Only the water data does not entirely overlap the data for the other materials, yet even so, the water data fall in a correlation line.

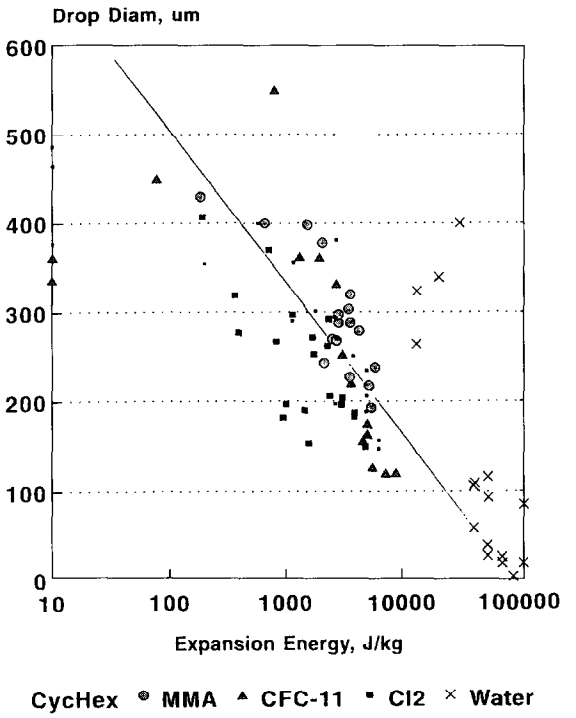

Fig. 9. Drop sizes which fit corrected rainout data as a function of expansion energy. The correlation line is given by $dp = 740 - 60.37 \ln E_{EXP}$.

(2) Using expansion energy as a correlator also provides a reasonably adequate fit, although a semi-logarithmic plot is needed. The water data are moved considerably to the right, as indicated in Table 7, but not out of proportion with the correlation line. Comparing Figs. 2 and 9, the corrected chlorine and methylamine data now fall nearer a correlation line. Since more data are used in Fig. 9, the scatter in the data is larger, but a larger range of overpressure is now included.

(3) Multiplying by the liquid heat capacity, and dividing by the heat of vaporization to plot drop size against the extended flash fraction, F_p, in Fig. 10 provides the only change in the set of correlators which moves water data to the left relative to CFC-11 data. The water data are made to overlap the data for chlorine, methylamine, and CFC-11. However, the cyclohexane data are moved farther right than any of the other components, as consistent with Table 7, and overlap the other component's data only at low values of F_p.

(4) Multiplying by the expansion ratio, ρ_L/ρ_v, to plot drop size against the Jacob number in Fig. 11 does not improve the correlation. The water data are moved far to the right (by about a factor of 6.5). The cyclohexane data are moved slightly to the left relative to CFC-11, which helps, but the CFC-11 data still fall left of data for the other materials.

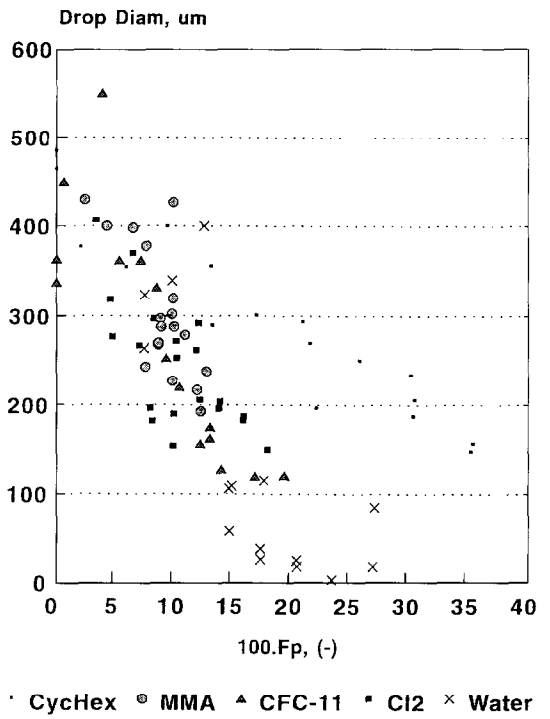

Fig. 10. Drop sizes which fit corrected rainout data as a function of the extended flash fraction.

(5) Multiplying by $(\pi\alpha)^{1/2}$ to plot drop size against the bubble growth rate, C_{bub}, as in Fig. 12 helps to bring the data closer for CFC-11, MMA, chlorine, and cyclohexane, but the water data are moved farther to the right. This correlation requires different correlation lines for water and the other materials, which does not alone rule out its utility.

8. Correlating drop size with overpressure

The effect of overpressure is considered in the additive terms in E_{exp}, F_p, and E_p. Only a few experiments were made in the CCPS tests which varied overpressure substantially with superheat essentially constant. These are listed in Table 8. Increasing discharge pressure decreases the expansion energy, which worsens the correlation. The data indicate rainout (and drop size) decrease with discharge pressure and with expansion energy. Physically, the expansion energy in going between P_o and P_{sat} is not exerting appreciable work against the atmosphere because the liquid specific volume remains unchanged in this pressure range. For these reasons, we propose defining the partial expansion energy and the extended flash fraction with an additive term involving overpressure, $P_o - P_{sat}$. This way, overpressure is recognized as available to breakup droplets.

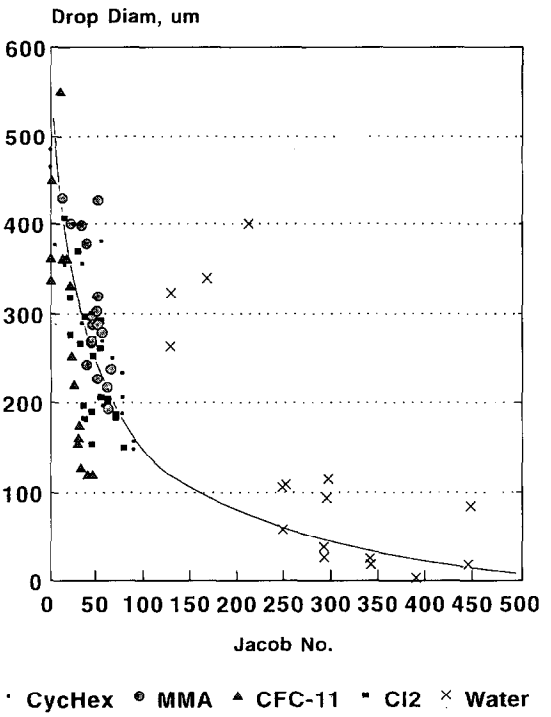

Fig. 11. Drop sizes which fit corrected rainout data as a function of Jacob number.

Unfortunately, the overpressure term makes a negligible contribution to the value of F_p. However, it does appreciably effect E_p. Fig. 13 shows that E_p provides the proper directional behavior for correlating with overpressure. In fact, in using E_p even the drop sizes for subcooled experiments are pulled into consistency with the correlation line in Fig. 14, which is an improvement over Fig. 9.

9. Conclusions

The CCPS rainout data for chlorine and methylamine have been corrected for evaporation using a model which accounts for the competition between dissolution and evaporation. The model requires specification of an adjustable parameter, the solubility of chlorine in caustic solution and the solubility of methylamine in acid solution. It predicts that an essentially constant fraction of the rained out liquid dissolves (35% of the chlorine and 89% of the methylamine).

The CCPS rainout data for cyclohexane have been corrected to account for all of the variables which significantly affect evaporation from the capture pans, including solar radiation, ambient temperature, droplet temperature, wind speed, and release

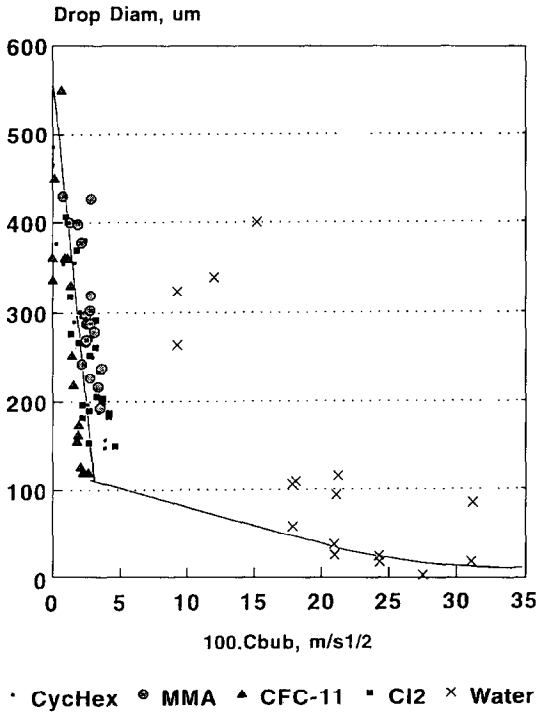

Fig. 12. Drop sizes which fit corrected rainout data as a function of bubble growth rate.

Table 6
Typical values of physical properties used in prospective drop size correlators

Material	T_{sat} (K) at 1 atm	T for property eval'n, (K)	C_{pL} (J/kg)	h_{fg} (kJ/kg)	ρ_L (kg/m^3)	ρ_v (kg/m^3)	ρ_L/ρ_v	α (m^2/s) $\times 10^4$
Chlorine	239.12	259.1	912.2	278.4	1510	3.390	445	7.191
MMA	266.8	286.8	3203	787.3	669.9	1.354	495	5.406
CFC-11	297.0	317.0	501.8	175.0	1431	5.423	264	4.77
Cyclohexane	353.9	373.9	2219	341.1	700.2	2.831	247	5.97
Water	373.2	393.2	4230	2223	966.9	0.5626	1718	6.27

duration. Within the limitations of available information, model predictions were shown to agree with a ground-level release test used to check on evaporation within the pan.

Drop sizes were found by matching predicted with observed capture rates for all five materials from the CCPS tests. Six alternative correlator variables were tested with these data. Acceptable correlations can be obtained using superheat, partial expansion energy, and the bubble growth rate. The latter requires a correlation with

Table 7
Effect of terms in prospective drop size correlation relative to CFC-11

Material	$\frac{C_{pL}}{C^*_{pL}}$	$\frac{C_{pL}/h_{fg}}{(C_{pL}/h_{fg})^*}$	$\frac{\rho_L/\rho_v}{(\rho_L/\rho_v)^*}$	$\left[\frac{\alpha}{\alpha^*}\right]^{1/2}$
Chlorine	1.83	1.15	1.69	0.95
MMA	6.38	1.42	1.88	0.86
CFC-11	1.0	1.0	1.0	1.0
Cyclohexane	4.42	2.27	0.935	0.76
Water	8.47	0.667	6.51	1.15

Table 8
Experimental cases in which overpressure varied significantly at constant superheat

Material test no.	Super heat (K)	Over pressure (kPa)	Corrected rainout (m%)	$P_o - P_a$ (kPa)	E_{exp} (J/kg)	100 F_P (—)	E_p (J/kg)
Chlor 06	25.2	53.2	51.0	213	1150	8.36	1221
Chlor 16	24.7	340.4	25.0	495.7	1014	8.26	1467
Chlor 17	25.2	672.4	14.2	832.2	954	8.51	1849
Chlor 20	31.0	0.0	36.3	205.6	1756	10.32	1756
Chlor 07	30.8	53.9	44.3	268.3	1715	10.27	1788
Chlor 18	30.5	337.5	26.0	548.8	1588	10.24	2041
Chlor 19	30.4	677.5	8.4	888.8	1474	10.32	2385
MMA 16	21.8	0	30.4	119.6	2876	9.01	2876
MMA 6	21.5	59.1	25.0	193.4	2750	8.90	2926
MMA 15	21.5	334.9	24.8	469.2	2528	8.95	3525

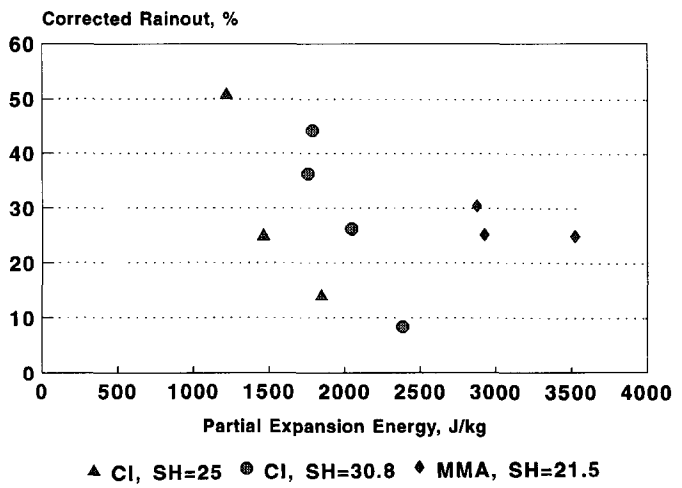

Fig. 13. Drop sizes for experiments in which overpressure was varied as a function of partial expansion energy.

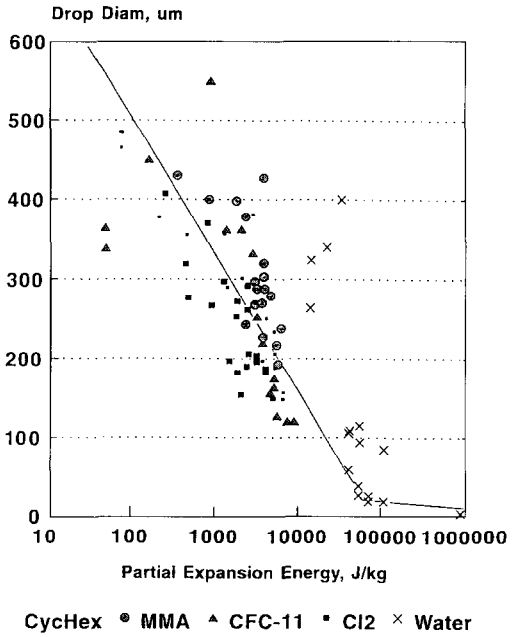

Fig. 14. Drop sizes which fit corrected rainout data as a function of partial expansion energy. The correlation is given by $dp = 722 - 57.33 \ln E_p$.

different line slopes for water and for the other four materials. We recommend the correlation obtained with partial expansion energy as providing the greatest overlap between data of the five materials. This correlator also has the right behavior with respect to overpressure.

Nomenclature

C_{bub}	bubble growth rate, $m\,s^{-1/2}$
C_{pL}	liquid heat capacity of condensable component, $J\,kg^{-1}K^{-1}$
Da^*	boundary layer Dalton number
d_p	droplet diameter, m
E_p	Partial expansion energy, $J\,kg^{-1}$
E_{exp}	expansion energy, $J\,kg^{-1}$
F_p	extended flash fraction, kg/kg
h_{fg}	heat of vaporization, at T_s, $J\,kg^{-1}$
h_{ni}	nonideal, pressure correction for vapor enthalpy, $J\,kg^{-1}$
ΔH	specific enthalpy change, $J\,kg^{-1}$
H_L	liquid specific enthalpy $J\,kg^{-1}$
H_v	vapor specific enthalpy, $J\,kg^{-1}$
Ja	Jacob number

k	thermal conductivity of the gas, $W\,m^{-1}K^{-1}$
m	mass in pool or cloud, kg
P_a	ambient pressure, Pa
P_o	stagnation pressure in tank, Pa
P_{sat}	vapor pressure, Pa
r	pool radius, m
S	solubility, kg solute/kg solvent
T_{atm}	ambient temperature, K
T_g	temperature of gas phase, K
T_d	temperature of drops, K
T_o	stagnation temperature, K
T_{ref}	reference temperature, K
T_{sat}	saturation temperature, K
ΔT_{sh}	superheat, K
T_2	temperature after expanding to atmospheric pressure along isentropic path, K
t	time, s
Δt	release duration, s
u_o	expansion zone velocity of jet, $m\,s^{-1}$
u_w	wind speed at 10 m height, $m\,s^{-1}$
v_o	specific volume of cloud, m^3kg^{-1}
We	Weber number
w	discharge rate, $kg\,s^{-1}$
w_s	Solubility, kg solute/kg solution $[S/(1+S)]$
w_∞	concentration of solute in background solution, kg/kg solution
x	mass fraction of flashed vapor

Greek letters

α	thermal diffusivity, $(k/C_p\rho)$, $m^2\,s^{-1}$
ρ_L	liquid density, $kg\,m^{-3}$
ρ_v	gas density, $kg\,m^{-3}$
ρ_{air}	density of ambient air, $kg\,m^{-3}$
ρ_w	density of water, $kg\,m^{-3}$
σ	surface tension, $N\,m^{-1}$

References

[1] Center for Chemical Process Safety, Final Report by Energy Analysts, Norman, OK, 90-03-540, available through AIChE, NY, 1989.

[2] Center for Chemical Process Safety, Final Report by Quest Consultants, Inc., Norman, OK, 91-12-6012, available through AIChE, NY, 1991.

[3] D.W. Johnson, Proc. Int. Conf. and Workshop on Modeling and Mitigating the Consequences of Accidental Releases of Hazardous Materials, New Orleans, LA, AIChE, CCPS, pp. 1–34, 20–24 May 1991.

[4] J.L. Woodward, A. Papadourakis and J. Cook, J. Hazard. Mater., 44 (1995) 185.
[5] J.L. Woodward and A. Papadourakis, Proc. Int. Conf. and Exhibition on Safety, Health, and Loss Prevention in the Oil, Chemical, and Process Industries, Singapore, 15–19 February 1993.
[6] F.T. Dodge, J.T. Park, J.C. Buckingham and R.J. Magott, US Coast Guard Report CG-D-35-83, Southwest Research Institute, June 1983.
[7] Center for Chemical Process Safety, Final Report by DNV Technica, Inc, Columbus, OH; available through AIChE, NY, February, 1995.
[8] Merck Index, 9th edn., Merck and Co., Rahway, NJ, pp. 2065–2066, 5882, 1976. (This gives solubility $S = 0.092$ mole Chlorine/liter of water and $S = 959\ m^3/m^3$ of MMA vapor.)
[9] National Climatic Data Center, National Oceanographic and Atmospheric Agency, US Dept. of Commerce, Asheville, NC, September 1992.
[10] J.H. Lienhard and J.B. Day, J. Basic Eng. Trans. AIME, (1970) 515.
[11] R. Brown and J.L. York, A.I.Ch.E. J., 8 (1962) 149–153.
[12] C.T. Crowe and W.J. Comfort, Proc. 1st Int. Conf. on Liquid Atomization and Spray Systems, Tokyo, Paper 2–3, 27–31 August 1978.
[13] Y. Kitamura, H. Morimitsu and T. Takahashi, Ind. Eng. Chem. Fundam., 25 (1986) 206–211.
[14] A. Koestel, R.G. Gido and D.E. Lamkin, NUREG/CR-1607, August 1980.
[15] D.M. Bushnell and P.B. Gooderum, J. Spacecraft, 5 (1968) 231–232.
[16] J.H. Lienhard and J.M. Stephenson, J. Basic Eng. Trans. ASME (1966) 525–532.
[17] G.A. Melhem and R. Saini, 1992 Process Plant Safety Symposium, Houston, TX, February 1992.